

Metabolomics to study the sublethal effects of diazepam and irbesartan on glass eels (*Anguilla anguilla*)

Iker Alvarez-Mora^{a,b,*}, Valérie Bolliet^c, Naroa Lopez-Herguedas^{a,b}, Maitane Olivares^{a,b}, Mathilde Monperrus^d, Nestor Etxebarria^{a,b}

^a Department of Analytical Chemistry, University of the Basque Country, Basque Country, Leioa Biscay 48080, Spain

^b Plentzia Marine Station, University of the Basque Country, Basque Country, Plentzia Biscay 48620, Spain

^c E2S UPPA, ECOBIOP, Aquapôle INRAE, MIRA, Université de Pau et des Pays de l'Adour, Saint-Pée-sur-Nivelle F64310, France

^d Institut des Sciences Analytiques et de Physico-chimie pour l'Environnement et les matériaux, Université de Pau et des Pays de l'Adour, Basque Country, Anglet 64000, France

ARTICLE INFO

Keywords:

Glass eels
Metabolomics
Mass spectrometry
Non-target analysis
Exposomics
Lipidomics

ABSTRACT

Since glass eels are continuously exposed to contamination throughout their migratory journey in estuaries, to a certain extent the fall in the population of this endangered species might be attributed to this exposure, which is especially acute in estuaries under high urban pressure. In this work, metabolomics was used to address the main objective of this study, to evaluate the effects of two pharmaceuticals previously identified as potential concerning chemicals for fish (diazepam and irbesartan) on glass eels. An exposure experiment to diazepam, irbesartan and their mixture was carried out over 7 days followed by 7 days of depuration phase. After exposure, glass eels were individually sacrificed using a lethal bath of anesthesia, and then an unbiased sample extraction method was used to extract separately the polar metabolome and the lipidome. The polar metabolome was submitted to targeted and non-targeted analysis, whereas for the lipidome only the non-targeted analysis was carried out. A combined strategy using partial least squares discriminant analysis and univariate and multivariate statistical analysis (ANOVA, ASCA, *t*-test, and fold-change analysis) was used to identify the metabolites altered in the exposed groups with respect to the control group. The results of the polar metabolome analysis revealed that glass eels exposed to the diazepam-irbesartan mixture were the most impacted ones, with altered levels for 11 metabolites, some of them belonging to the energetic metabolism, which was confirmed to be sensitive to these contaminants. Additionally, the dysregulation of the levels of twelve lipids, most of them with energetic and structural functions, was also found after exposure to the mixture, which might be related to oxidative stress, inflammation, or alteration of the energetic metabolism.

1. Introduction

The migratory cycle of the European eel (*Anguilla anguilla*) remains one of the least known behaviours in the animal kingdom. Adult eels spawn in the Sargasso Sea and the leptocephali (i.e., the larvae stage) drift with the Gulf Stream to reach the European continental shelf (Wright et al., 2022), where they metamorphose and turn into the so-called glass eel. In their second migratory phase, glass eels migrate up estuaries to join rivers, taking advantage of the current during the upstream flood tide and hiding in the estuarine bed during ebb tide (Gas-cuel, 1986). Along the estuarine migration, glass eels undergo several changes including morphological, physiological, and behavioural

changes (Elie and Rochard, 1994), as well as pigmentation process (Elie et al., 1982), gut development, osmotic adaptations (Ciccotti et al., 1993), and hormonal modifications (Jegstrup and Rosenkilde, 2003). However, these processes are often dependent on the intrinsic conditions of each individual (e.g. energy status and body conditions) (Liu et al., 2019) and several studies have described partial migratory patterns with less than a 20% of the glass eels migrating (Beaulaton and Castelnaud, 2005). Although many studies have aimed to understand the two migratory phenotypes (i.e., active glass eels that are able to use the tide to migrate efficiently, and inactive ones that settle in estuaries) (Liu et al., 2019), an accepted physiological explanation is still pending.

The energetic conditions of glass eels, as described by Claveau and

* Corresponding author: Department of Analytical Chemistry, University of the Basque Country, Basque Country, Leioa Biscay 48080, Spain.

E-mail address: iker.alvarez@ehu.eus (I. Alvarez-Mora).

<https://doi.org/10.1016/j.aquatox.2023.106547>

Received 25 February 2023; Received in revised form 12 April 2023; Accepted 25 April 2023

Available online 26 April 2023

0166-445X/© 2023 The Author(s). Published by Elsevier B.V. This is an open access article under the CC BY license (<http://creativecommons.org/licenses/by/4.0/>).

co-workers (Claveau et al., 2015), and contamination, could also influence this migratory behaviour. Likewise, the European eel shows environmental sex determination, and estuarine migration influences sexual differentiation (Davey and Jellyman, 2005; Harrison et al., 2014). Thus, although the uneven distribution of males and females at different heights in the estuary is a fact that has been described prior to this population decline, factors that may influence migration may further accentuate this disparity and influence reproduction. Furthermore, the glass eels are specially affected by contamination since they are directly exposed to contaminants released into estuaries from human activity (e.g., wastewater effluents), thus, the protection of this endangered species also relies on the evaluation of the contaminants present in these sensitive environments.

In this vein, previous works by our research group have tried to address the fate of contaminants of emerging concern (CECs) in the Adour estuary (Bayonne, Basque Country, France), which it is one of the main habitats for this species. In 2017, the three main wastewater treatment plants (WWTPs) that release their effluents into the estuary were studied and the quantification of contaminants included in the Water Framework Directive (WFD) was performed (Cavalheiro et al., 2017). More recently, the environmental risk assessment study led to the identification of diazepam, irbesartan and propranolol among the most remarkable CECs released by the WWTP of Bayonne (Alvarez-Mora et al., 2022). Precisely, the anxiolytic diazepam and the antihypertensive irbesartan were two of the compounds found at the highest concentration ($\sim 3 \text{ ng}\cdot\text{mL}^{-1}$) and it was also proven by a 7-day exposure experiment that they have a bioconcentration potential of up to 10-fold ($\text{BCF} = 10$). Furthermore, the biotransformation (i.e., metabolization potential of the selected contaminants by glass eels) of the compounds was also studied and a bioactive metabolite of diazepam, nordiazepam, was identified. Undoubtedly, the findings of this work are environmentally very relevant since the prioritization of potential contaminants allowed us to focus our efforts on a few candidates. But, although we were then able to experimentally prove the capacity of bioaccumulation and biotransformation, our previous work lacks to demonstrate empirically that the chosen pollutants do indeed produce a visible effect on the health of elvers. Therefore, this second study builds on that research base and uses metabolomics to try to answer this question.

Metabolomics is often used in toxicology to find the biochemical pathways disturbed by a stressing event (e.g., disease, nutritional imbalance, contaminant exposure...), because the search of altered small endogenous metabolites ($< 1.5 \text{ kDa}$) can provide a clear insight into the health status of an organism. In fact, environmental-metabolomics has been successfully applied to explore the cause-effect mechanisms of CECs in aquatic organisms (Colás-Ruiz et al., 2022; Labine et al., 2022; Xu et al., 2022; Ziarrusta et al., 2019) and it is one of the key elements in adverse outcome pathways (Brockmeier et al., 2017; Dumas et al., 2022).

Consequently, this work aims to provide metabolomic evidence on the effect that some significant contaminants found in this estuary can have on glass eels. Therefore, as a follow-up to the previous study on the fate of CECs in glass eels, the aim of this work was to investigate the effects of diazepam and irbesartan on the glass eel metabolic system. As mentioned above, irbesartan and diazepam were selected based on the observations of previous environmental risk assessment studies (Alvarez-Mora et al., 2022), and the exposure experiments were designed taking into account both previous studies (Alvarez-Mora et al., 2022; Ziarrusta et al., 2019) and the specificities of glass eels (Figueiredo et al., 2020; Liu et al., 2019). The exposure experiments were carried out at the concentrations found in the effluent in the previous study, which would refer to the worst-case scenario (Lopez-Herguedas et al., 2021), as we do not take into account the dilution factor that may be present in the estuary. Therefore, the precautionary principle is applied, justified by the input from the other two wastewater treatment plants discharging into the same estuary, and the changing dilution factor in the estuary depending on the water level. The alterations on the metabolic profile

were determined by means of a target and non-target analysis of the polar metabolome and non-target analysis of the lipidome through liquid chromatography coupled to high resolution mass spectrometry.

2. Experimental section

2.1. Standards and reagents

Information regarding the chemical standards used in the targeted analysis is provided in the supplementary information file (in Table SI.1). The list includes a wide range of metabolites representative of the main biochemical pathways usually assessed in environmental metabolomics. Diazepam and irbesartan standards were acquired from Sigma-Aldrich (St. Louis, MO, USA). HPLC grade methanol (MeOH), water, acetonitrile (ACN) and 2-propanol (IPA) were obtained from PanReac AppliChem (Barcelona, Spain). HPLC grade tert-butyl methyl ether (MTBE) was obtained from Sigma-Aldrich (St. Louis, MO, USA). MS grade formic acid (98% purity) and ammonium formate salt ($\geq 99\%$ purity) were purchased from Fisher Scientific (Madrid, Spain) and Fluka (Steinheim, Germany), respectively.

2.2. Fish collection

Procedures used in this study were validated by the ethics committee N°073 'Aquitaine Poissons-Oiseaux' (ref: APAFIS #32,100–2,021,062,317,263,102 v2). The experiment was carried out in strict accordance with the EU legal frameworks, specifically those relating to the protection of animals used for scientific purposes (i.e., Directive 2010/63/EU), and under the French legislation governing the ethical treatment of animals (Decret no. 2013–118, February 1st, 2013).

The sampling site is located at the estuarine mouth of a small river (French Basque coast France: 43.857822, -1.390253 , map available in Bolliet et al. (2017)). The fish were collected in December using a dip-net at night and during flood tide. Once collected, fish were transferred to the laboratory and maintained at $12 \pm 0.5 \text{ }^\circ\text{C}$ overnight in a tank containing aerated water from the fishing site. During the next week, 1/3 of the water was daily replaced by freshwater previously aerated during 24 h. The room was maintained under a photoperiod of 10 h of light / 14 h of darkness, with a very low light intensity during the photophase ($0.2\text{--}0.3 \mu\text{W}/\text{cm}^2$). After this transition to freshwater, a batch of 60 glass eels were used in this work.

2.3. Exposure conditions to assess the effects of diazepam and irbesartan on glass eels

A graphical overview of the setup used for contaminant exposure is shown in Fig. 1. Briefly, glass eels were exposed to diazepam and irbesartan at a nominal concentration of $3 \text{ ng}\cdot\text{mL}^{-1}$ ($10.5 \text{ nmol}\cdot\text{L}^{-1}$ and $7.0 \text{ nmol}\cdot\text{L}^{-1}$, respectively) pumping the 4 L contaminant solutions (diazepam, irbesartan and irbesartan + diazepam mixture) using a multi-channel peristaltic pump. This concentration agreed with that found in the effluent of the wastewater treatment plant that discharges its waste into the estuary and is the same concentration used in the previous work to determine bioaccumulation and biotransformation. Contaminant dosing solutions were prepared by dissolving the corresponding chemical in water carried by a minimum amount of MeOH ($< 0.1\%$). At the same time, two control tanks were prepared: the first one pumping water from an osmotic water reservoir that was renewed periodically, and a second MeOH control tank where MeOH was added using the same pump as for the contaminants to obtain the same expected concentration as in the exposure tanks. Twelve glass eels were introduced in each of the five tanks, all equipped with shelters for glass eels to hide. The temperature and photoperiod were maintained at $12 \text{ }^\circ\text{C}$ and a photoperiod of 10 h of light / 14 h of darkness along the whole experiment, which took 14 days (7 days of exposure and 7 days of depuration). Water, diazepam, and irbesartan flows, as well as water temperature, were

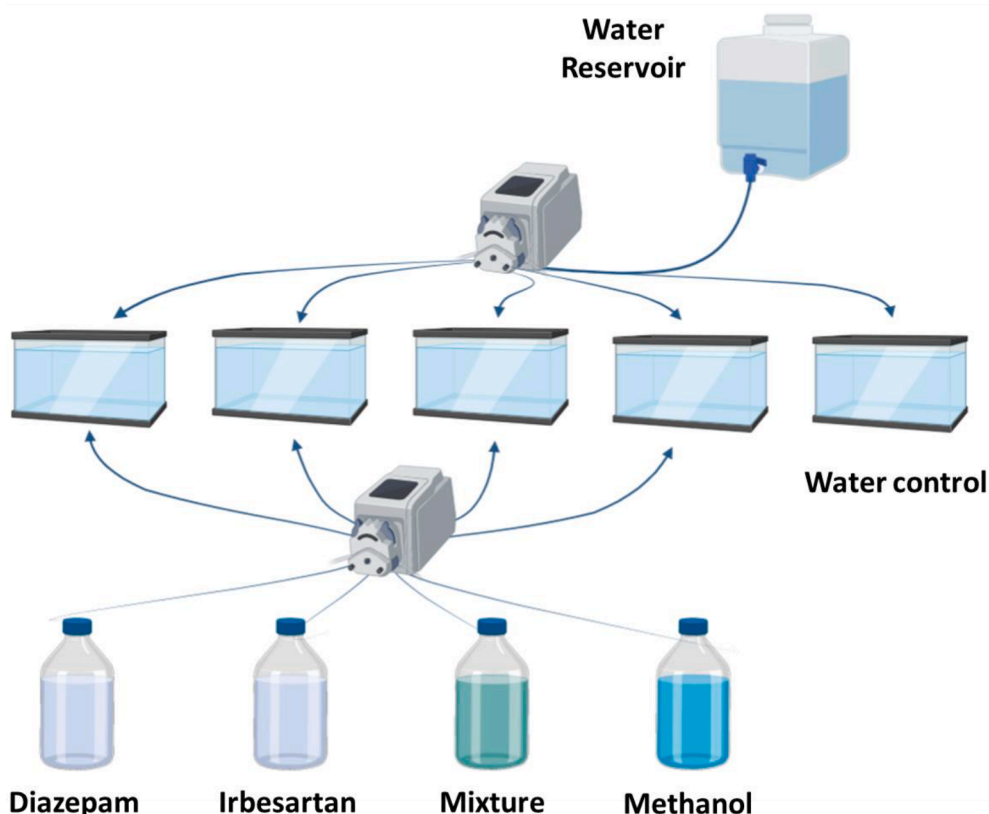


Fig. 1. Set-up used for the exposure experiments of glass eels to diazepam and irbesartan. Two multichannel peristaltic pumps were used, one peristaltic to supply the tanks with osmotic water and the second one to pump the different contaminants into the corresponding tanks.

checked daily during the 7 days of exposure to avoid any sharp fluctuations in the nominal concentrations. The stability of the exposure set-up was tested in the previous work by Alvarez-Mora (2022) and co-workers. Glass eels ($n = 6$ individuals) were collected after 7 days of exposure and after 7 days of depuration. This way the experimental groups were defined as follows: two control groups (C7 & C14), two diazepam-exposed groups (D7 & D14), two irbesartan-exposed groups (I7 & I14), two diazepam-irbesartan-exposed groups exposed to the mix of both contaminants (DI7 & DI14), and two groups exposed to the expected MeOH concentration (MC7 & MC14). Glass eels were anaesthetized, sacrificed using a lethal bath of anesthesia (benzocaine, 0.01 mg L^{-1}), individually measured for the wet weight ($\pm 1.0 \text{ mg}$) and length ($\pm 0.5 \text{ mm}$), and then flash-frozen in liquid nitrogen and stored at $-80 \text{ }^\circ\text{C}$ before analysis.

2.5. Metabolite extraction

The analysed samples were whole glass eel bodies previously cut into pieces with a scalpel to facilitate homogenisation ($\sim 300 \text{ mg}$, see Table SI.2). The sample extraction was carried out via an unbiased extraction approach based on a two-phase extraction system (Chen et al., 2013). Briefly, $300 \mu\text{L}$ MeOH and $100 \mu\text{L}$ of water (UHPLC-MS quality) were added to the samples before being homogenized ($6400 \text{ rpm} - 60 \text{ s} \times 3 - 15 \text{ s}$) (Precellys®, Bertin Instruments, Montigny-le-Breonneux, France) at $4 \text{ }^\circ\text{C}$ using homogenization tubes with ceramic beads (1.0 mm diameter). Thereafter, $900 \mu\text{L}$ MTBE and $250 \mu\text{L}$ water were added and the homogenization process was repeated (Chen et al., 2013). The extracts were centrifuged for 5 min ($4 \text{ }^\circ\text{C}$, $21,000 \text{ G}$) (Allegra X-30R Centrifuge, Beckman Coulter®), the solid fraction was removed and the liquid centrifuged for 15 min (Ribbenstedt et al., 2018) to get two phases (organic phase and aqueous phase), which were collected separately. The organic phase was evaporated under N_2 flow

(XcelVap®) until dryness, redissolved in 1.5 mL IPA:MeOH:water (4:3:1) mixture (Paglia and Astarita, 2017) and diluted with the same solvent for injection (1:10, v/v). The polar phase was collected and diluted directly (1:10 and 1:50) using a mixture of water:methanol (3:1, v/v). For qualitative quality control purposes, a pool containing small aliquots ($20 \mu\text{L}$) from all the extracts ($n = 30$) was also prepared.

2.6. UHPLC Q-Orbitrap analysis

Sample analysis was carried out using a Dionex Ultimate 3000 UHPLC (Thermo Scientific) coupled to a Q-Exactive Focus hybrid quadrupole-Orbitrap MS (Thermo Scientific, Waltham, Massachusetts, United States) with a heated electrospray ionization source, (HESI, Thermo, CA, USA). The separation of metabolites present in the polar phase was done by injecting aliquots of $5 \mu\text{L}$ onto a Kinetex® C_{18} ($2.6 \mu\text{m}$, 100 \AA , LC Column $150 \times 3 \text{ mm}$; Precolumn SecurityGuard® ULTRA Cartridges UHPLC C_{18} 2.1 mm) chromatographic column maintained at $35 \text{ }^\circ\text{C}$. HPLC Water and HPLC Water:AcN 5:95 (each containing 10 mM Ammonium formate or 0.1% Formic acid for negative or positive mode respectively) were used as mobile phase A and B, respectively, and the separation was conducted at 0.3 mL/min using the following gradient conditions: $0 \text{ min } 5\% \text{ B}$; $1 \text{ min } 5\% \text{ B}$; $15 \text{ min } 95\% \text{ B}$; $20 \text{ min } 95\% \text{ B}$; $24 \text{ min } 5\% \text{ B}$. Regarding the analysis of non-polar phase, $5 \mu\text{L}$ -aliquots were injected in a Luna® Omega C_{18} ($1.6 \mu\text{m}$, 100 \AA , LC Column $150 \times 2.1 \text{ mm}$) chromatographic column. The separation was done at $35 \text{ }^\circ\text{C}$ using as mobile phases A: $60\% \text{ ACN}$ in water and B: IPA:ACN (9:1), both containing 10 mM ammonium formate and 0.1% formic acid in both positive and negative modes, respectively (Chen et al., 2013). The gradient used in this case was as follows: $0 \text{ min } 40\% \text{ B}$; $3 \text{ min } 70\% \text{ B}$; $10 \text{ min } 100\% \text{ B}$; $22 \text{ min } 100\% \text{ B}$; $27 \text{ min } 50\% \text{ B}$; $28 \text{ min } 50\% \text{ B}$ with a flow rate of 0.2 mL/min . The ionization conditions in the HESI were the followings: the sheath and the auxiliary gas flow rates were established

at 55 and 10 units respectively, the ion spray voltage was 3.10 kV for positive ionization and 3.20 kV for negative, and temperatures were kept at 300 °C for the capillary and 290 °C for the auxiliary gas heater. Data were acquired using the full scan data dependant MS2 (Full-Scan-dd-MS2) mode, where the full scan range was fixed between m/z 50–750 for polar compounds and m/z 70–1000 for non-polar ones with a resolution of 70 000 in the Full MS scan. Three ddMS2-scans were completed for every full scan with a resolution of 17 500. In addition, the quality control pools were injected

2.7. Data handling

For the targeted analysis of the polar metabolome, data were processed using Trace Finder 5.1 (Thermo Scientific). The integration of the chromatographic peak areas was carried out by the automatic function using the Intelligent Component Integration System (ICIS) algorithm. The correct integration was evaluated metabolite by metabolite over the calibration solutions. The non-targeted screening of metabolites was performed using Compound Discoverer 3.3 (Thermo-Fisher Scientific, Waltham, MA, USA). Features were detected following the non-targeted metabolomics workflow, as broadly described by Gonzalez-Gaya et al. (González-Gaya et al., 2021), using a mass tolerance of 5 ppm and a minimum peak intensity of 10^5 . All the metabolomic features found were matched with freely available MS mass lists such as HMDB 5.0 (Wishart et al., 2022), LipidMaps (Fahy et al., 2007), and the endogenous metabolite database from Compound Discoverer and mzCloud MS libraries. Additionally, from the resulting list of candidates, a manual inspection was carried out to remove either noisy peaks or non-meaningful peaks (bad chromatographic shape, poor fragmentation), and only features with peak areas 10 times larger in samples than blanks were further considered. Through the Fish Scoring application, the *in-silico* fragmentation of the final list of candidates was run to include the match level among the quality metrics. The statistical handling of the filtered data was carried out by MetaboAnalyst (v5.0) (Pang et al., 2022). PLS-DA was followed by statistical tests (ANOVA, corrected *t*-tests for multiple comparisons and fold change analysis) to explore the effect of the different conditions and discover the altered metabolites. ASCA (ANOVA Simultaneous Component Analysis (Pérez-Cova et al., 2022) and ANOVA2 were used to study more than one factor simultaneously. In parallel, to assess the robustness of the PLS-DA models was assessed using the PLS-Toolbox (v8.9.1, Eigenvector Research), where receiver operating characteristic (ROC) curves were also created.

3. RESULTS and discussion

3.1. Analysis of the polar metabolome

The polar metabolome was analysed by target and non-target approaches. In the former case, we were able to quantify 40 polar metabolites in the glass-eels as shown in Table SI.3. In the non-target approach, many of the previously quantified metabolites were also annotated according to the confidence levels proposed by Schymanski et al. (2014). In addition to these, 12 metabolites were also annotated as level 2a, and 6 as level 3. The data resulting from both screening methods (target analysis and levels 2a and 3 of the nontarget analysis) were merged, log transformed and autoscaled to homogenize the scale differences between concentrations and peak areas (from target and non-target screening respectively). Quality control samples were used to exclude all the metabolites showing an $RSD_{Area} > 40\%$ in the non-target screening.

The underlying rationale is that the study and the analysis of slight modifications in the metabolic profile would provide key information regarding chemical events that happen after the exposure to the selected contaminants and not any other confounding factor. To ensure the right application of this approach, we should assure that most of the

remaining factors that might modify the metabolomic profile are kept constant (Villas-Boas et al., 2007; Bedia, 2022). This means that the experiments should be carefully designed taking into account the sources of variation and minimizing the effect of all the non-controlled ones (e.g., the effect of methanol as carrier). As previously mentioned, two of the main sources of variation in this kind of studies, sex and feeding, are not influential since the sex of glass eels is still not defined and they fast until the juvenile stage (Van Wichelen et al., 2022).

On the other hand, during the design of exposure experiments two assumptions were considered and tested to minimize the effect of two non-controlled variables: (i) the proportion of methanol required to dissolve diazepam and irbesartan stock solutions would not affect metabolic profile, and (ii) the expected variations from 7 to 14 days in control tanks would be random within the experimental uncertainty. To confirm those two assumptions, we first analysed the data obtained from the two control tanks (one with water and the other with the expected MeOH level) at the two exposure times (7 and 14 days). The data was treated using Metaboanalyst through the statistical analysis with meta-data application and using both two-way ANOVA and ASCA. The ASCA method is perfectly suited for designed multivariate data to distinguish the effect of treatments. The metrics used to select the most significant metabolites or to show the goodness of the model have been the false discovery rate (FDR or *q*-level) when ANOVA or *t*-test was used, the *p*-value for ASCA model validation and the R^2 and Q^2 to check the robustness of the biased classification methods (PLS-DA). FDR is a method used to control the proportion of false positives when multiple hypothesis tests are conducted. In metabolomics, where large numbers of measurements are taken, the use of a *p*-value threshold alone to determine significance can result in many false positives.

The ASCA model was validated with 200 permutations and exposure time was statistically significant (*p*-level < 0.05), suggesting that the glass-eels metabolome was altered during the exposure without the need of any other chemical stressor. In fact, levels of tryptophan, creatinine, fructose 1,6-diphosphate, isoleucine, pipercolinic acid and 8-hydroxydeoxyguanosine were altered along the experiment in control tank. In the case of the interaction between the methanol effect and exposure time (i.e., the net effect of the combination of treatment and time, and which may give us clues about the synergistic effects of these two variables) the significant metabolites were: reduced glutathione, acetyl- and butyryl-L-carnitine. These conclusions were also confirmed using ANOVA2, which showed that 21 metabolites were significant (see Table SI.4) for the exposure time and only one was significant for the interaction between the exposure time and the methanol effect. Therefore, the C7 and C14 sets of data could not be pooled in a single group. A better visualization of this differences of both groups is provided by the scores plot of the PLS-DA model (Fig. 2), where the variable importance in projection (VIP) plot also shows the most relevant metabolites for class differentiation. The robustness of the model can be checked via the R^2 and Q^2 values and ROC curves in Table SI.5 and Table SI.6. The PLS-DA model clearly differentiates the two conditions and this fact is confirmed through the corrected *t*-test for multiple comparisons that showed that the levels of the first two metabolites in the VIP plot (i.e., tryptophan and creatinine) are significantly (*q*-value = 0.081) lower in C14 (Table SI.7). The time-dependent effect was also observed in other exposure experiment set-ups carried out with fish (Ziarrusta et al., 2019), probably due to the different number of fish present in the tank along the experiment. In this case, since glass eels are fasting, we could think that the metabolism might show a kind of depletion effect in some of the metabolites. Therefore, we have to consider exposure time as a key factor per se and to interpret the net effect of the contaminants we should take this effect into account.

From these preliminary observations, we can also confirm that the concentration of methanol used in this work does not have any effect on the metabolic profile of the glass eels. This was definitely demonstrated by the *t*-test (adjusted by the FDR) of these two groups, which showed no significant differences (Table SI.8). This outcome agrees with that

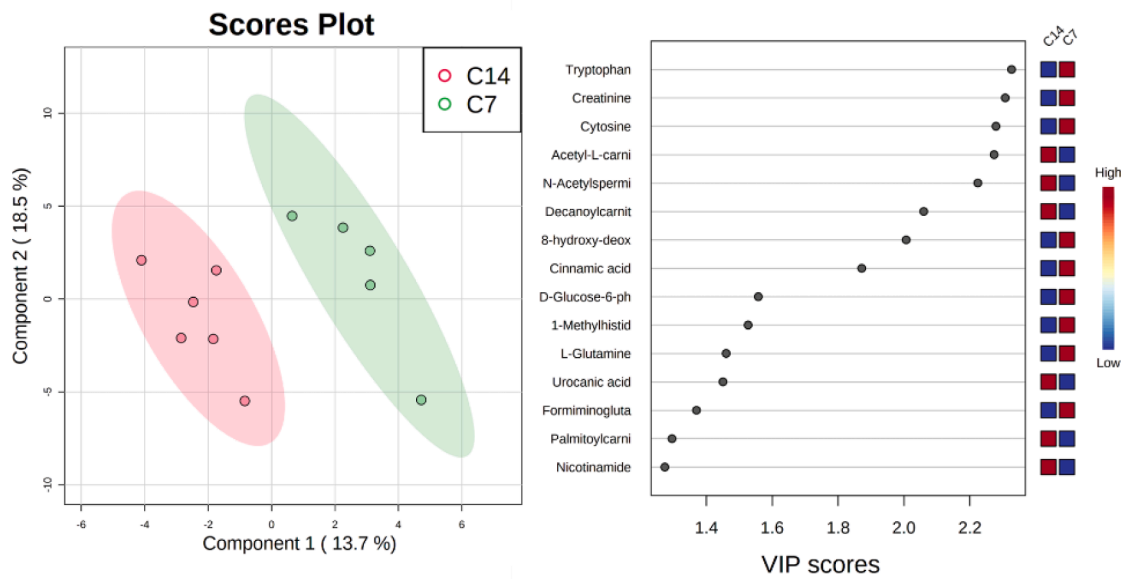


Fig. 2. The PLS-DA scores plot of the polar metabolites of the control groups at two sampling times (left) shows a clear differentiation of the experimental groups, mainly explained by the metabolites at the top of the VIP scores (right).

reported by Maes et al. (2012), where the authors highlight the suitability of methanol to deliver contaminants in exposure experiments.

In order to avoid the influence of the exposure time on the analysis, we compared the exposed tank and the control one at the same exposure time (i.e., D7 vs C7 and D14 vs C14) to, first, (i) study the effect of the contaminants compared to the control after 7 days of exposure, and second, (ii) in the case that the contaminant effect was confirmed, to assess whether the metabolic levels match the control group after the depuration phase.

First of all, we compared the three exposure conditions by means of a PLS-DA analysis, as shown in Fig. 3, to determine whether the exposure

to the selected contaminants (D, I and DI at 7 days) had any impact in the disturbance of the polar metabolic profile of glass eels. The cluster distance between control samples and the exposed samples can give us insight into the degree of their impact. As seen in Fig. 3, the diazepam and irbesartan mixture showed the highest distance from controls and, although the classification metrics R^2 and Q^2 do not show a great performance of the model (as only one of the groups shows differences), the ROC curves from cross-validation confirmed that this group was completely differentiated from the rest (Table SI.6). Although the sum of both drug concentrations can be the simplest explanation for this, we cannot discard the option of synergic effects. Moreover, an impact

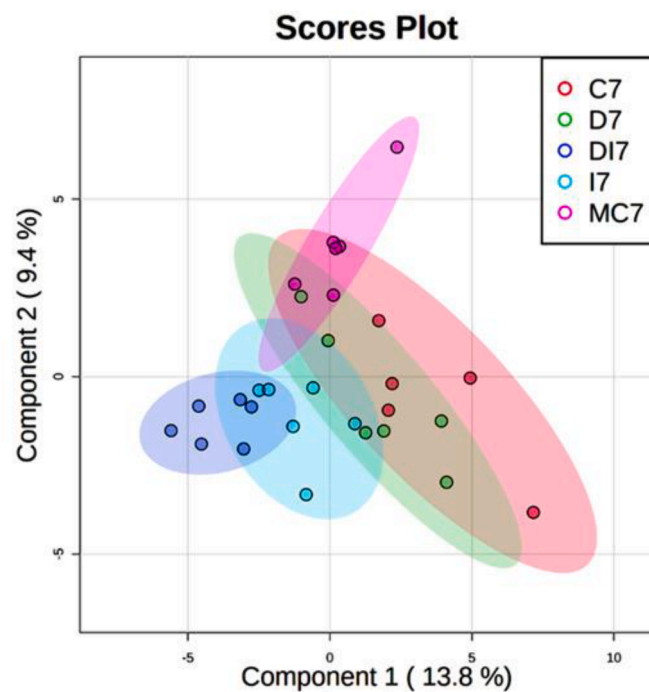


Fig. 3. The PLS-DA scores plot of the identified metabolites for all the experimental condition at day 7 shows that although the experimental groups cannot all be distinguished from each other, there is a tendency for the exposed groups to move away from the control, with DI7 being the furthest away.

gradient can be retrieved from the PLS-DA scores plot with diazepam exposed samples barely differentiating from controls and irbesartan overlapping between controls and the mixture.

Since the highest differences were expected to happen in the combined exposure to irbesartan and diazepam, we analysed the Control 7–14 days and Diazepam-Irbesartan 7–14 days set of data by means of the ANOVA2 and ASCA analysis, as described before. Briefly, since it was demonstrated that no significant differences were observable between C7 and MC7, we merged both types of controls to enhance the statistical significance, and we proceeded with the analysis with log-transformed and autoscaled data to give equal weight to all the variables and get a normally distributed dataset. On the one hand, the ANOVA analysis showed that 10 metabolites (concretely, *N*-Acetylhistidine, glutathione oxidized (GSSH), carnosine, 2-methylbutyrylcarnitine, isovalerylcarnitine, adenosine 5'-monophosphate (AMP), hexanoylcarnitine, guanine, 8-hydroxy-deoxyguanosine and fructose 1,6-diphosphate) were statistically significant (p-level < 0.05) in the interaction between exposure time and exposure type (the mixture diazepam-irbesartan). On the other hand, the ASCA model validated with 200 permutations showed that the treatment and the exposure time were not statistically significant (p-level 0.15 and 0.09, respectively) but the interaction was significant (p-level = 0.025) being 5 metabolites (concretely, AMP, adenosine triphosphate (ATP), guanine, GSSH and 8-hydroxy-deoxyguanosine) responsible of such difference. The boxplots of all the metabolites matching between both approaches are shown in Table SI.9.

Additionally, the *t*-test comparison of DI7 vs C7 samples revealed that 2 metabolites were significantly altered (q-value = 0.017 & 0.025 respectively) for AMP and D-glucose-6-phosphate. The fold-change analysis showed that L-citrulline and adenosine levels were also remarkably reduced after the contaminant mixture exposure (fold-change < 2) and the levels of urocanic acid increased (fold-change > 2) (Fig. 4.A). The heat maps depicting the metabolites altered by diazepam, irbesartan and the mixture can also be found in Table SI.10.

The effectiveness of the depuration phase was checked comparing each exposure condition to the control group. After 7 days of depuration only urocanic acid recovered control levels, whereas the effect on L-Citrulline levels was inverted (Fig. 4.B). Therefore, we can conclude that 7 days is an insufficient period for the glass eels to recover their basal condition, but a longer study would be necessary to be able to conclude whether the effects are permanent or not.

3.2. Interpretation of polar metabolomic profiles

In the case of the control and exposure time comparison, the different profiles observed for the control groups at different exposure times were

related to the variation in two amino acids (tryptophan and phenylalanine), two metabolites (pipecolinic acid from lysine and 8-hydroxydeoxyguanosine from 2'-deoxyguanosine), a phosphosugar (fructose 1,6-diphosphate). From the pathway analysis option in Metaboanalyst, these results suggest an impact in the metabolism of certain amino acids using the KEGG pathway library for fish (*Danio rerio*). As shown in Fig. 5, the circles in the metabolome view graphic represent the matched pathways, where the pathway impact value corresponds to the number of metabolites identified within a given pathway, and the y-axis indicates whether the metabolites involved in those pathways are significantly altered or not. The depletion of the amino acid reserves (observed at C14) together with a higher oxidation of fatty acids (increase of acetylcarnitine in D14) might suggest the adaptation to the fasting conditions. It is worth mentioning that most of the amino acids highlighted in this work are considered either ketogenic (lysine), glucogenic (histamine, threonine) or both (phenylalanine, tryptophan) and therefore they can be oxidized through the tricarboxylic acid (TCA) cycle (Falco et al., 2020). Dietary uptake is the main source of the essential amino acids tryptophan and phenylalanine in fish, so that we cannot rule out that the drop in concentrations over time is simply related to the lack of uptake, i.e., fasting, since it cannot be synthesized in their organism. In addition, since the experiment involved the analysis of the whole organism, the role of the microbiome cannot be discarded.

Regarding the effects of the diazepam-irbesartan mixture on glass eels metabolism, the search for the toxicological mechanisms of pollutants including diazepam and irbesartan would lead us to expect an increase in oxidative stress and DNA damage due to the generation of more reactive oxygen species (ROS) after diazepam exposure (Blahová et al., 2013; Ogueji et al., n.d.), which would lead to increased protein denaturation and changes in the activities of antioxidant enzymes, as well as altering the levels of other biochemical parameters such as glutathione peroxidase, catalase, alanine aminotransferase, aspartate aminotransferase, alkaline phosphatase, protein and glucose metabolism (Ogueji et al., n.d.; Pereira et al., 2013). In the particular case of diazepam, since this compound acts on GABA receptors, alterations on the GABA metabolic pathway would also be expected. Since diazepam and irbesartan have very different MoAs, we think that it is most likely a synergic effect than an additive one (Liess et al., 2020), regardless the fact that in the exposure to the mixture we double the total concentration, but further dose-response analysis would have been required. Finally, although the role of controls is to cancel most of the unwanted effects, we could also consider some confounding effects based on the use of wild eels. For instance, some contaminants may have not been thoroughly removed during the acclimation period (Alvarez-Mora et al., 2022), and therefore, the observed effects might be the consequence of

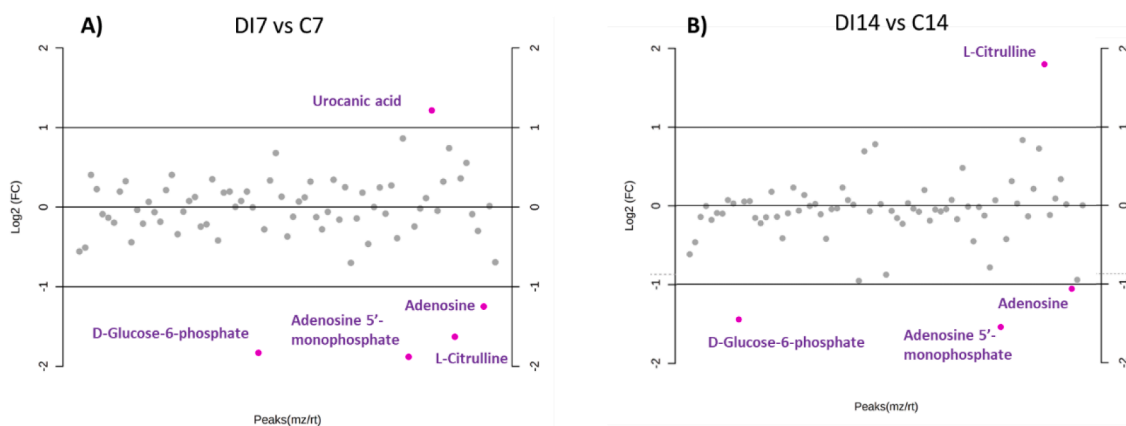


Fig. 4. Results of the fold change analysis of A) DI7 vs C7 and B) DI14 vs C14. Coloured and out of the -1 to 1 interval are the metabolites showing fold change values higher or lower than the 2.0 or 0.5 thresholds respectively (i.e., 2-fold difference between conditions).

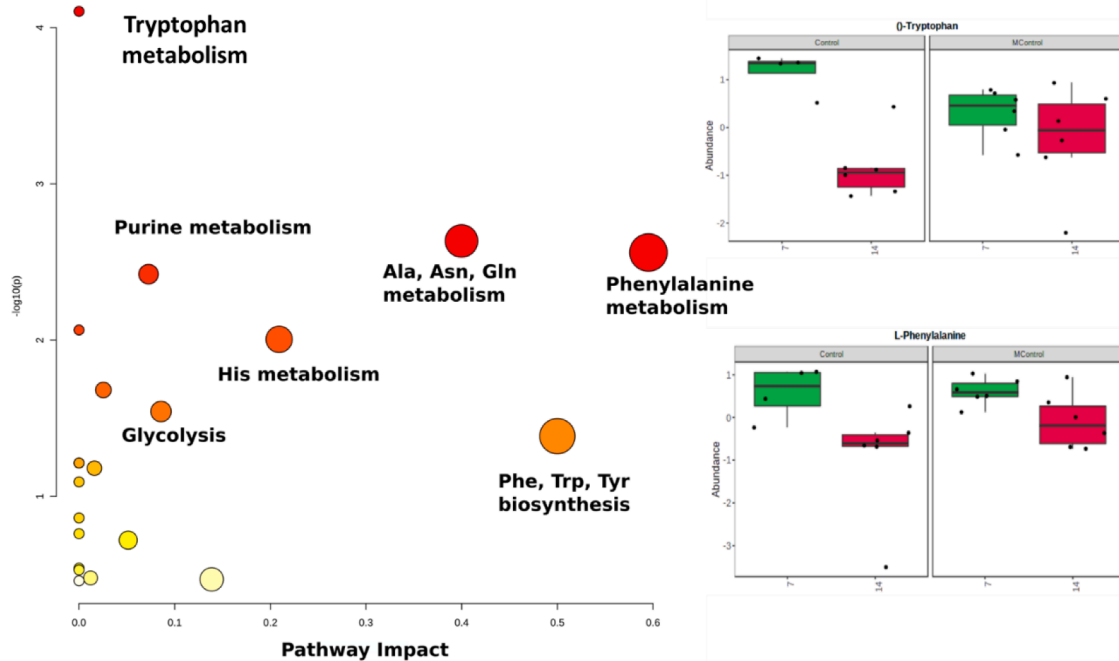


Fig. 5. Pathway analysis of the identified metabolites in C7 vs C14 (left). color intensity is linked to the relevance of that pathway in the condition differentiation and the size of the circle to % of identified metabolites within the pathway. The main altered pathways observed were the tryptophan metabolism, phenylalanine metabolism and the alanine, asparagine and glutamine metabolism. In the right, box plot of the selected significant metabolites: tryptophan and L-Phenylalanine.

some of those conceal contaminants together with the exposed ones (e. g., pharmaceuticals such as exemestane, primidone, iloprost, or norethandrolone).

In this work, the altered metabolites were identified by the comparison of the different exposure tanks (i.e. 7 and 14 independently) with their respective control tank in order to eliminate the time-dependent factor. The impacted pathways after 7 days of exposure and 7 days of depuration are shown in Figs. 6A and 6B, respectively. The presence of the mixture of drugs affected mainly histidine and b-alanine metabolism and in a lesser extent glycolysis and purine metabolism. All the altered metabolites belonging to those pathways show systematically lower concentrations in the fish of dosed tank in comparison to the control ones. As for the metabolic pathways significantly altered after depuration, glycolysis, purine and fructose metabolism stick out. The VIP plot from both day 7 also shows that systematically lower concentrations are found in the exposed glass eels, whereas at day 14 the trend changes for 6 of the main altered metabolites but still lower concentrations can be found for oxidized glutathione, ATP, and two acylcarnitines.

Overall, combining the outcome of the univariate and the multivariate analysis, the results suggest that the most affected metabolites were the nucleotides ATP and AMP involved in the energy regulation of cells; the purine, purine nucleosides and purine metabolite guanine, adenosine, guanosine, 8-hydroxydeoxyguanosine; the intracellular form of glucose, G6P; the α -amino acid citrulline; the intermediate in the L-histidine catabolism, urocanic acid; and the antioxidant tripeptide glutathione reduced. AMP, ATP and G6P are metabolites related to the energy metabolism and sensitive indicators of energy stress. The energetic equilibrium of cells is regulated by the reaction $2ADP \leftrightarrow ATP + AMP$ which is driven towards ADP in unstressed cells (Hardie, 2014). Adenosine is produced in the cell through the hydrolysis of AMP, therefore, is not surprising that a higher availability of AMP would lead to higher concentrations of adenosine. This metabolite plays an important role in protecting against cell damage and combating organ dysfunction (Borea et al., 2016). G6P acts as the central hub of the carbohydrate metabolism (Rajas et al., 2019) and it works as substrate for the different metabolic pathways involved in energy production.

According to the observations found in this work, we can state that the energy metabolism is sensitive to the contaminant mixture. Furthermore, it is also noteworthy the downregulation of the purine metabolism and in particular the guanine-based purines. Although the mechanism of these metabolites is not yet fully understood, some studies confirmed that purines have important roles in the nervous system, including the modulation of the glutamatergic system, a common role shared by diazepam (Cao et al., 2014; Schmidt et al., 2007). Therefore, we can affirm that there is a correlation between the exposure to the contaminant mixture and some metabolic changes, however the mechanism behind these changes is still unknown and should be further investigated.

3.3. Lipidome analysis

Although spectral match cannot assure the exact isomer among many candidates with equivalent structures, 221 lipids were annotated by non-target screening, most of them at level 3 (Table SI.11). Since a wide range of the identified lipids correspond to phospholipids with at least one unsaturated fatty acid, distinguishing between positional isomers becomes unfeasible, thus, the generic name was given to these lipids (i. e., the position of the double bond is not specified) and they were classified within the identification confidence level 3.

The statistical analysis was carried out following the workflow described before. Initially, as shown in Fig. 7, a PLS-DA screening was applied to evaluate the distribution of the scores and the differences between conditions. The first two latent variables were able to discriminate the C7 from DI7 (LV1) and C7 from D7 (LV2). Unlike in the polar metabolome, where the metabolite disturbance was reflected in a single latent variable, here two sources of variability seem to appear. Somehow, D7 and DI7 affect the lipidome in independent ways, disturbing the concentration levels of different lipids. For day 14, the separation between groups DI14 and C14 was not observed, suggesting that the impact that the mix of diazepam and irbesartan has in the lipidome can no longer be observed since none of the more than 200 metabolites is significantly different between these groups.

Nonetheless, even though diazepam showed no significant effect at

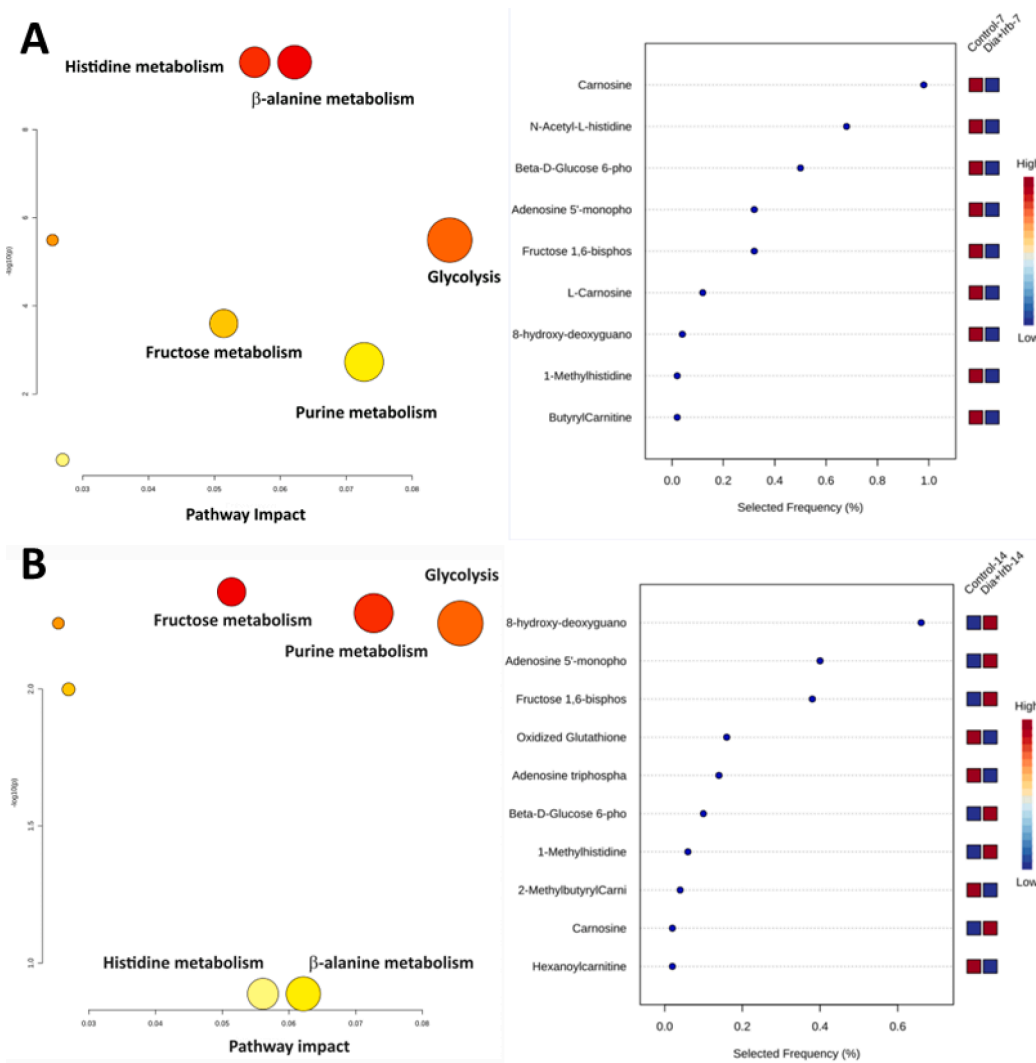


Fig. 6. Pathway analysis of the identified metabolites in DI7 vs C7 (A) and DI14 vs C14 (B) and their related VIP scores plots showing the main altered metabolites from the treatment and time interaction. For time 7, the histidine and alanine metabolisms as well as the glycolysis were the main altered pathways, whereas for time 14, while the glycolysis pathway remained altered, fructose and purine metabolisms gained importance.

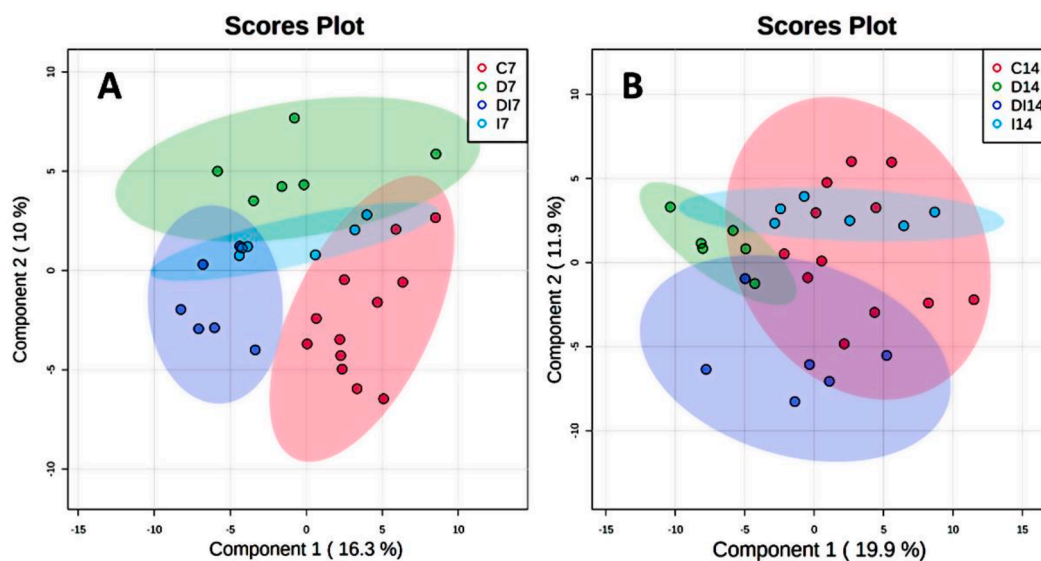


Fig. 7. PLS-DA scores plot of the identified lipids for all the conditions at day 7 (A) and day 14 (B). At day 7, DI7 and D7 can be differentiated from C7 while I7 remains overlapped in the midst of all. At day 14 no clear differentiation could be observed.

day 7, the statistical analysis hints that there might be a rebound effect seeing that the levels of 4 metabolites were altered after the depuration phase (D14 vs C14).

A more detailed analysis of the Control vs DI at 7 and 14 days was accomplished by means of the ANOVA2 and ASCA procedures, and the significant lipids are listed in Table 1. According to ANOVA2, 6 metabolites were significant (p -level < 0.05) for the treatment (tank) and 6 more for both the interaction between exposure time and the treatment. The ASCA model was carried out with 1 PCs for the type of treatment, exposure time and the interaction of both. This model was validated with 200 permutations showing that only the interaction was clearly significant (p -level < 0.05) but the independent factors showed a slight significant level (both $p \sim 0.08$). Although the systemic disruption of any of the lipid families cannot be demonstrated, we can affirm that the contaminant mix can alter the levels of some specific lipids.

3.4. Interpretation of the altered Lipidome

The results of the lipidomic analysis identified that the concentration levels of 7 lipids were significantly disturbed from C7 to DI7. The most striking compound was ceramide d18:1/22:0 (C22) which appeared enhanced up to six times in the exposed group. Ceramides were first thought to be mere structural elements or intermediates in the synthesis or metabolism of all the sphingolipids, but they are also important in the intra- and inter- cellular signaling (Turpin-Nolan and Brüning, 2020) and in the blood pressure control (Spijkers et al., 2011). Hence, the exposure of glass eels to the anti-hypertensive irbesartan may be related to the abnormal ceramide levels observed in DI7, which were also observed in I7.

PCs and PEs are the most common phospholipids found in cell membranes. There are important precursors for a range of highly biologically active mediators of metabolism and physiology and phospholipids remodeling is certainly involved in homeoviscous adaptation of biological membranes, especially in temperature adaptation (Tocher et al., 2008). The low PC/PE ratios found in DI7 can influence energy metabolism and can be linked to liver disease progression (van der Veen et al., 2017), even though this has only been proven in mammals and the extrapolation to fish could be too daring. At the same time, increased levels of LPC are related to pro-inflammatory status in fish and mammals (Aiyar et al., 2007; Tocher et al., 2008). Finally, the presence of high levels of oxidized phospholipids (e.g. LPC-O) is usually related to conditions of oxidative stress (Bochkov et al., 2010). Juvenile of Atlantic salmon exposed to long term handling stress showed an increase in concentration of oxidized phosphatidylcholines that may result of the breakdown of phosphatidylcholine and be used as a biomarker of long term stress in fish (Karakach et al., 2009). Here, the ratio of LPC-O could be another indicator of the metabolic stress that was observed in the control group. Phosphatidic acids (PA) are less abundant lipids that is used as the main building block for the synthesis of other diacylglycerols and triacylglycerols and thus play an important structural role (Tanguy et al., 2019). It is also worth mentioning the relationship between this lipid family and the central nervous system since PAs have been shown to have signaling activity and alterations in PA dynamics have been related to neurological disorders such as neurodegeneration (Oliveira et al., 2010) or neurological cancer (Park et al., 2009) in

Table 1
Significantly altered lipids identified by either ASCA and ANOVA2 approaches.

FAMILY	COMPOUNDS
Ceramides	Cer (18:1/22:0)
Triacylglycerols (TG)	TG (16:0/16:1/17:0), TG (17:0/17:1/17:1)
Lyso-Phosphatidylcholines (LPC)	LPC 22:6, LPC O-16:0, LPC O-18:0
phosphatidic acids (PA)	PA (17:0/22:6)
Phosphatidylcholines (PC)	PC (18:5/24:6)
Phosphatidylethanolamines (PE)	PE (18:1/0:0), PE (21:0/0:0), PE (20:0/19:1)

studies using mammalian cell lines, but much more work is still needed to elucidate the role of these lipids in fish metabolism. Finally, triacylglycerols are responsible of storing the excess of fatty acids in cell and the activation of TG biosynthesis protects cells from membrane damage under oxidative stress (Li et al., 2018). The significantly higher concentration of these lipids in DI7 could be explained as a defense mechanism to fight the oxidative stress provoked by the exposure.

4. Conclusions

Since glass eels are continuously exposed to contamination throughout their migratory journey through the estuaries, the decline in the population of this endangered species might be to some extent due to the exposure to contaminants, which is especially acute in estuaries under high urban pressure. Although there is still a long way to go to prove this statement, this study adds to the long list of work demonstrating the harmful effects of certain CECs on aquatic organisms and shows the usefulness of metabolomics in this field for the discovery of novel bioindicators that can complement the existing ones. By means of exposure experiments and metabolomic profiling, we have assessed the effects of two of the most relevant contaminants released to the Adour estuary on glass eels' metabolome. An exposure experiment to diazepam, irbesartan and their mixture at the concentration levels found in effluent WWTP, simulating the worst-case scenario, was carried out over 7 days followed by 7 days of depuration phase. Based on the observations, the mixture of both contaminants had the highest impact on glass eels, altering the metabolic levels of 2 metabolites. Adenosine 5'-monophosphate and D-glucose-6-phosphate showed remarkably reduced concentrations after the exposure, which suggests that the energetic metabolism is sensitive to the contaminant mixture. The lipidomic analysis also revealed that the concentrations of seven lipids were also altered after the exposure to this mixture, confirming that both the polar metabolome and the lipidome are affected by this mixture. However, before we can confirm what our results suggest, we believe it is important to support this hypothesis using other methodological approaches that allow us to see the same effect at different physiological levels. For now, we can say that the combination of the results present in this and our previous work (Alvarez-Mora et al., 2022) gives us a broad picture of the impact that contaminants can have on glass eels from their fate within the glass eel organism to the sublethal effects, supports the implementation of metabolomics as a complementary tool in the evaluation of toxicological effects, and provides further evidence of the need to improve the efficiency of wastewater treatment processes, especially for the contaminants of emerging concern.

CRedit authorship contribution statement

Iker Alvarez-Mora: Conceptualization, Methodology, Investigation, Formal analysis, Writing – original draft, Writing – review & editing, Visualization. **Valérie Bolliet:** Conceptualization, Methodology, Investigation, Resources, Writing – review & editing, Supervision, Project administration, Funding acquisition. **Naroa Lopez-Herguedas:** Methodology, Investigation, Formal analysis, Writing – review & editing. **Maitane Olivares:** Data curation, Writing – review & editing. **Mathilde Monperrus:** Resources, Conceptualization, Writing – review & editing, Supervision, Project administration. **Nestor Etxebarria:** Conceptualization, Methodology, Investigation, Resources, Writing – original draft, Writing – review & editing, Supervision, Project administration, Funding acquisition.

Declaration of Competing Interest

The authors declare that they have no known competing financial interests or personal relationships that could have appeared to influence the work reported in this paper.

Data availability

Data will be made available on request.

Acknowledgments

Authors acknowledge financial support from the Agencia Estatal de Investigación (AEI) of Spain and the European Regional Development Fund through CTM2017–84763-C3–1-R and CTM2020–117686RB-C31 projects and the Basque Government through the financial support as a consolidated group of the Basque Research System (IT1446–22). Nara Lopez-Herguedas is grateful to the Spanish Ministry of Economy, Industry and Competitiveness for her predoctoral scholarship FPI 2018. Iker Alvarez-Mora is grateful to the University of the Basque Country and the Université de Pau et des Pays de L' Adour for his cotutelle predoctoral scholarship.

Supplementary material

Supplementary material associated with this article can be found, in the online version, at doi [10.1016/j.aquatox.2023.106547](https://doi.org/10.1016/j.aquatox.2023.106547).

References

- Aiyar, N., Disa, J., Ao, Z., Ju, H., Nerurkar, S., Willette, R.N., Macphee, C.H., Johns, D.G., Douglas, S.A., 2007. Lysophosphatidylcholine induces inflammatory activation of human coronary artery smooth muscle cells. *Mol. Cell. Biochem.* 295, 113–120. <https://doi.org/10.1007/s11010-006-9280-x>.
- Alvarez-Mora, I., Bolliet, V., Lopez-Herguedas, N., Castro, L., Anakabe, E., Monperrus, M., Etxebarria, N., 2022. Prioritization based on risk assessment to study the bioconcentration and biotransformation of pharmaceuticals in glass eels (*Anguilla anguilla*) from the Adour estuary (Basque Country, France). *Environ. Pollut.* 311, 120016 <https://doi.org/10.1016/j.envpol.2022.120016>.
- Beaulaton, L., Castelnaud, G., 2005. The efficiency of selective tidal stream transport in glass eel entering the Gironde (France). *Bull. Fr. Pêche Piscic.* 5–21. <https://doi.org/10.1051/kmae:2005001>.
- Bedia, C., 2022. Metabolomics in environmental toxicology: applications and challenges. *Trends Environ. Anal. Chem.* 34, e00161. <https://doi.org/10.1016/j.teac.2022.e00161>.
- Blahová, J., Pihlavová, L., Hostovský, M., Divišová, L., Dobsíková, R., Mikulíková, I., Stěpanová, S., Svobodová, Z., 2013. Oxidative stress responses in zebrafish *Danio rerio* after subchronic exposure to atrazine. *Food Chem. Toxicol. Int. J. Publ. Br. Ind. Biol. Res. Assoc.* 61, 82–85. <https://doi.org/10.1016/j.fct.2013.02.041>.
- Bochkov, V.N., Oskolkova, O.V., Birukov, K.G., Levonen, A.L., Binder, C.J., Stöckl, J., 2010. Generation and Biological Activities of Oxidized Phospholipids. *Antioxid. Redox Signal.* 12, 1009–1059. <https://doi.org/10.1089/ars.2009.2597>.
- Bolliet, V., Claveau, J., Jarry, M., Gonzalez, P., Baudrimont, M., Monperrus, M., 2017. Migratory behavior, metabolism, oxidative stress and mercury concentrations in marine and estuarine European glass eels (*Anguilla anguilla*). *Physiol. Behav.* 169, 33–40. <https://doi.org/10.1016/j.physbeh.2016.11.008>.
- Borea, P.A., Gessi, S., Merighi, S., Varani, K., 2016. Adenosine as a multi-signalling guardian angel in human diseases: when, where and how does it exert its protective effects? *Trends Pharmacol. Sci.* 37, 419–434. <https://doi.org/10.1016/j.tips.2016.02.006>.
- Brockmeier, E.K., Hodges, G., Hutchinson, T.H., Butler, E., Hecker, M., Tollefsen, K.E., Garcia-Reyero, N., Kille, P., Becker, D., Chipman, K., Colbourne, J., Collette, T.W., Cossins, A., Cronin, M., Graystock, P., Gutsell, S., Knapen, D., Katsiadaki, I., Lange, A., Marshall, S., Owen, S.F., Perkins, E.J., Plaistow, S., Schroeder, A., Taylor, D., Viant, M., Ankley, G., Falciani, F., 2017. The role of omics in the application of adverse outcome pathways for chemical risk assessment. *Toxicol. Sci.* 158, 252–262. <https://doi.org/10.1093/toxsci/kfx097>.
- Cao, L., Bie, X., Huo, S., Du, J., Liu, L., Song, W., 2014. Effects of diazepam on glutamatergic synaptic transmission in the hippocampal CA1 area of rats with traumatic brain injury. *Neural. Regen. Res.* 9, 1897–1901. <https://doi.org/10.4103/1673-5374.145357>.
- Cavalheiro, J., Zuloaga, O., Prieto, A., Preudhomme, H., Amouroux, D., Monperrus, M., 2017. Occurrence and fate of organic and organometallic pollutants in municipal wastewater treatment plants and their impact on receiving waters (Adour Estuary, France). *Arch. Environ. Contam. Toxicol.* 73, 619–630. <https://doi.org/10.1007/s00244-017-0422-9>.
- Chen, S., Hoene, M., Li, J., Li, Y., Zhao, X., Häring, H.U., Schleicher, E.D., Weigert, C., Xu, G., Lehmann, R., 2013. Simultaneous extraction of metabolome and lipidome with methyl tert-butyl ether from a single small tissue sample for ultra-high performance liquid chromatography/mass spectrometry. *J. Chromatogr. A* 1298, 9–16. <https://doi.org/10.1016/j.chroma.2013.05.019>.
- Ciccotti, B.E., Macchi, E., Rossi, A., Cataldi, E., Cataudella, S., 1993. Glass eel (*Anguilla anguilla*) acclimation to freshwater and seawater: morphological changes of the digestive tract. *J. Appl. Ichthyol.* 9, 74–81. <https://doi.org/10.1111/j.1439-0426.1993.tb00528.x>.
- Claveau, J., Monperrus, M., Jarry, M., Pinaly, H., Baudrimont, M., Gonzalez, P., Amouroux, D., Bardonnet, A., Bolliet, V., 2015. Spatial and seasonal variations of methylmercury in European glass eels (*Anguilla anguilla*) in the Adour estuary (France) and relation to their migratory behaviour. *Environ. Sci. Pollut. Res.* 22, 10721–10732. <https://doi.org/10.1007/s11356-015-4303-3>.
- Colás-Ruiz, N.R., Ramírez, G., Courant, F., Gomez, E., Hampel, M., Lara-Martín, P.A., 2022. Multi-omic approach to evaluate the response of gilt-head sea bream (*Sparus aurata*) exposed to the UV filter sulisobenzone. *Sci. Total Environ.* 803, 150080 <https://doi.org/10.1016/j.scitotenv.2021.150080>.
- Davey, A.J.H., Jellyman, D.J., 2005. Sex determination in freshwater eels and management options for manipulation of sex. *Rev. Fish Biol. Fish.* 15, 37–52. <https://doi.org/10.1007/s11160-005-7431-x>.
- Dumas, T., Courant, F., Fenet, H., Gomez, E., 2022. Environmental metabolomics promises and achievements in the field of aquatic ecotoxicology: viewed through the pharmaceutical lens. *Metabolites* 12, 186. <https://doi.org/10.3390/metabo12020186>.
- Elie, P., Lecomte-Finiger, R., Cantrelle, I., Charlon, N., 1982. Définition des limites des différents stades pigmentaires durant la phase civelle d' *Anguilla anguilla* L. (Poisson Téléostéen Anguilliforme). *Vie Milieu* 32, 149–157.
- Elie, P., Rochard, E., 1994. Migration des civelles d'anguilles (*Anguilla anguilla* L.) dans les estuaires, modalités du phénomène et caractéristiques des individus. *Bull. Fr. Pêche Piscic.* 81–98. <https://doi.org/10.1051/kmae:1994006>.
- Fahy, E., Sud, M., Cotter, D., Subramaniam, S., 2007. LIPID MAPS online tools for lipid research. *Nucleic. Acids. Res.* 35, W606–W612. <https://doi.org/10.1093/nar/gkm324>.
- Figueiredo, C., Raimundo, J., Lopes, A.R., Lopes, C., Rosa, N., Brito, P., Diniz, M., Caetano, M., Grilo, T.F., 2020. Warming enhances lanthanum accumulation and toxicity promoting cellular damage in glass eels (*Anguilla anguilla*). *Environ. Res.* 191, 110051 <https://doi.org/10.1016/j.envres.2020.110051>.
- Gascuel, D., 1986. Flow-carried and active swimming migration of the glass eel (*Anguilla anguilla*) in the tidal area of a small estuary on the French Atlantic coast. *Helgol. Mar. Res.* 40 (3), 321–326. <https://doi.org/10.1007/BF01983739>.
- González-Gaya, B., Lopez-Herguedas, N., Santamaría, A., Mijangos, F., Etxebarria, N., Olivares, M., Prieto, A., Zuloaga, O., 2021. Suspect screening workflow comparison for the analysis of organic xenobiotics in environmental water samples. *Chemosphere* 274, 129964. <https://doi.org/10.1016/j.chemosphere.2021.129964>.
- Hardie, D.G., 2014. AMP-activated protein kinase: a key regulator of energy balance with many roles in human disease. *J. Intern. Med.* 276, 543–559. <https://doi.org/10.1111/joim.12268>.
- Harrison, A.J., Walker, A.M., Pinder, A.C., Briand, C., Aprahamian, M.W., 2014. A review of glass eel migratory behaviour, sampling techniques and abundance estimates in estuaries: implications for assessing recruitment, local production and exploitation. *Rev. Fish Biol. Fish.* 24, 967–983. <https://doi.org/10.1007/s11160-014-9356-8>.
- Jegstrup, I.M., Rosenkilde, P., 2003. Regulation of post-larval development in the European eel: thyroid hormone level, progress of pigmentation and changes in behaviour. *J. Fish Biol.* 63, 168–175. <https://doi.org/10.1046/j.1095-8649.2003.00138.x>.
- Karakach, T.K., Huenupi, E.C., Soo, E.C., Walter, J.A., Afonso, L.O.B., 2009. 1H-NMR and mass spectrometric characterization of the metabolic response of juvenile Atlantic salmon (*Salmo salar*) to long-term handling stress. *Metabolomics* 5, 123–137. <https://doi.org/10.1007/s11306-008-0144-0>.
- Labine, L.M., Oliveira Pereira, E.A., Kleywegt, S., Jobst, K.J., Simpson, A.J., Simpson, M.J., 2022. Comparison of sub-lethal metabolic perturbations of select legacy and novel perfluorinated alkyl substances (PFAS) in *Daphnia magna*. *Environ. Res.* 212, 113582 <https://doi.org/10.1016/j.envres.2022.113582>.
- Li, N., Sancak, Y., Frasor, J., Atilla-Gokcumen, G.E., 2018. A protective role for triacylglycerols during. *Apoptosis. Biochem.* 57, 72–80. <https://doi.org/10.1021/acs.biochem.7b00975>.
- Liess, M., Henz, S., Shahid, N., 2020. Modeling the synergistic effects of toxicant mixtures. *Environ. Sci. Eur.* 32, 119. <https://doi.org/10.1186/s12302-020-00394-7>.
- Liu, H., Labonne, J., Coste, P., Huchet, E., Plagnes-Juan, E., Rives, J., Veron, V., Seiliez, I., Bolliet, V., 2019. Looking at the complex relationships between migration behavior and conditional strategy based on energy metabolism in the European glass eel (*Anguilla anguilla*). *Sci. Total Environ.* 696 <https://doi.org/10.1016/j.scitotenv.2019.134039>.
- Lopez-Herguedas, N., González-Gaya, B., Castelblanco-Boyacá, N., Rico, A., Etxebarria, N., Olivares, M., Prieto, A., Zuloaga, O., 2021. Characterization of the contamination fingerprint of wastewater treatment plant effluents in the Henares River Basin (central Spain) based on target and suspect screening analysis. *Sci. Total Environ.* 151262 <https://doi.org/10.1016/j.scitotenv.2021.151262>.
- Maes, J., Verlooy, L., Buenafe, O.E., Witte, P.A.M., Esguerra, C.V., Crawford, A.D., 2012. Evaluation of 14 organic solvents and carriers for screening applications in zebrafish embryos and larvae. *PLOS One* 7, e43850. <https://doi.org/10.1371/journal.pone.0043850>.
- E.O. Ogueji, S.C. Iheanacho, C.D. Nwani, C.E. Mbah, O.C. Okeke, I.B. Usman, n.d. Toxicity of Diazepam On Lipid peroxidation, Biochemical and Oxidative Stress Indicators On Liver and Gill Tissues of African catfish *Clarias gariepinus* (Burchell, 1822).
- Oliveira, T.G., Chan, R.B., Tian, H., Laredo, M., Shui, G., Staniszewski, A., Zhang, H., Wang, L., Kim, T.-W., Duff, K.E., Wenk, M.R., Arancio, O., Paolo, G.D., 2010. Phospholipase D2 ablation ameliorates alzheimer's disease-linked synaptic dysfunction and cognitive deficits. *J. Neurosci.* 30, 16419–16428. <https://doi.org/10.1523/JNEUROSCI.3317-10.2010>.

- Paglia, G., Astarita, G., 2017. Metabolomics and lipidomics using traveling-wave ion mobility mass spectrometry. *Nat. Protoc.* 12, 797–813. <https://doi.org/10.1038/nprot.2017.013>.
- Pang, Z., Zhou, G., Ewald, J., Chang, L., Hacariz, O., Basu, N., Xia, J., 2022. Using MetaboAnalyst 5.0 for LC-HRMS spectra processing, multi-omics integration and covariate adjustment of global metabolomics data. *Nat. Protoc.* 1–27. <https://doi.org/10.1038/s41596-022-00710-w>.
- Park, M.H., Ahn, B.H., Hong, Y.K., Min, D.S., 2009. Overexpression of phospholipase D enhances matrix metalloproteinase-2 expression and glioma cell invasion via protein kinase C and protein kinase A/NF- κ B/Sp1-mediated signaling pathways. *Carcinogenesis* 30, 356–365. <https://doi.org/10.1093/carcin/bgn287>.
- Pereira, L., Fernandes, M.N., Martinez, C.B.R., 2013. Hematological and biochemical alterations in the fish *Prochilodus lineatus* caused by the herbicide clomazone. *Environ. Toxicol. Pharmacol.* 36, 1–8. <https://doi.org/10.1016/j.etap.2013.02.019>.
- Pérez-Cova, M., Platikanov, S., Stoll, D.R., Tauler, R., Jaumot, J., 2022. Comparison of multivariate ANOVA-based approaches for the determination of relevant variables in experimentally designed metabolomic studies. *Mol. Basel Switz.* 27, 3304. <https://doi.org/10.3390/molecules27103304>.
- Rajas, F., Gautier-Stein, A., Mithieux, G., 2019. Glucose-6 phosphate, a central hub for liver carbohydrate metabolism. *Metabolites* 9, 282. <https://doi.org/10.3390/metabo9120282>.
- Ribbenstedt, A., Ziarrusta, H., Benskin, J.P., 2018. Development, characterization and comparisons of targeted and non-targeted metabolomics methods. *PLOS One* 13, e0207082. <https://doi.org/10.1371/journal.pone.0207082>.
- Schmidt, A.P., Lara, D.R., Souza, D.O., 2007. Proposal of a guanine-based purinergic system in the mammalian central nervous system. *Pharmacol. Ther.* 116, 401–416. <https://doi.org/10.1016/j.pharmthera.2007.07.004>.
- Schymanski, E.L., Jeon, J., Gulde, R., Fenner, K., Ruff, M., Singer, H.P., Hollender, J., 2014. Identifying Small Molecules via High Resolution Mass Spectrometry: communicating Confidence. *Environ. Sci. Technol.* 48, 2097–2098. <https://doi.org/10.1021/es5002105>.
- Spijkers, L.J.A., Janssen, B.J.A., Nelissen, J., Meens, M.J.P.M.T., Wijesinghe, D., Chalfant, C.E., De Mey, J.G.R., Alewijnse, A.E., Peters, S.L.M., 2011. Antihypertensive treatment differentially affects vascular sphingolipid biology in spontaneously hypertensive rats. *PLoS One* 6, e29222. <https://doi.org/10.1371/journal.pone.0029222>.
- Tanguy, E., Wang, Q., Moine, H., Vitale, N., 2019. Phosphatidic Acid: from Pleiotropic Functions to Neuronal Pathology. *Front. Cell. Neurosci.* 13.
- Tocher, D.R., Bendiksen, E.Å., Campbell, P.J., Bell, J.G., 2008. The role of phospholipids in nutrition and metabolism of teleost fish. *Aquaculture* 280, 21–34. <https://doi.org/10.1016/j.aquaculture.2008.04.034>.
- Turpin-Nolan, S.M., Brüning, J.C., 2020. The role of ceramides in metabolic disorders: when size and localization matters. *Nat. Rev. Endocrinol.* 16, 224–233. <https://doi.org/10.1038/s41574-020-0320-5>.
- van der Veen, J.N., Kennelly, J.P., Wan, S., Vance, J.E., Vance, D.E., Jacobs, R.L., 2017. The critical role of phosphatidylcholine and phosphatidylethanolamine metabolism in health and disease. In: *Biochim. Biophys. Acta BBA Biomembr. Membr. Lipid Ther. Drugs Target. Biomembr.*, 1859, pp. 1558–1572. <https://doi.org/10.1016/j.bbmem.2017.04.006>.
- Van Wichelen, J., Verhelst, P., Perneel, M., Van Driessche, C., Buysse, D., Belpaire, C., Coeck, J., De Troch, M., 2022. Glass eel (*Anguilla anguilla* L. 1758) feeding behaviour during upstream migration in an artificial waterway. *J. Fish Biol.* 101, 1047–1057. <https://doi.org/10.1111/jfb.15171>.
- Villas-Boas, S.G., Nielsen, J., Smedsgaard, J., Hansen, M.A.E., Roessner-Tunali, U., 2007. *Metabolome Analysis: An Introduction*. John Wiley & Sons.
- Wishart, D.S., Guo, A., Oler, E., Wang, F., Anjum, A., Peters, H., Dizon, R., Sayeeda, Z., Tian, S., Lee, B.L., Berjanskii, M., Mah, R., Yamamoto, M., Jovel, J., Torres-Calzada, C., Hiebert-Giesbrecht, M., Lui, V.W., Varshavi, D., Varshavi, D., Allen, D., Arndt, D., Khetarpal, N., Sivakumaran, A., Harford, K., Sanford, S., Yee, K., Cao, X., Budinski, Z., Liigand, J., Zhang, L., Zheng, J., Mandal, R., Karu, N., Dambrova, M., Schiöth, H.B., Greiner, R., Gautam, V., 2022. HMDB 5.0: the human metabolome database for 2022. *Nucleic. Acids. Res.* 50, D622–D631. <https://doi.org/10.1093/nar/gkab1062>.
- Wright, R.M., Piper, A.T., Aarestrup, K., Azevedo, J.M.N., Cowan, G., Don, A., Gollock, M., Rodriguez Ramallo, S., Velterop, R., Walker, A., Westerberg, H., Righton, D., 2022. First direct evidence of adult European eels migrating to their breeding place in the Sargasso Sea. *Sci. Rep.* 12, 15362. <https://doi.org/10.1038/s41598-022-19248-8>.
- Xu, M., Legradi, J., Leonards, P., 2022. Using comprehensive lipid profiling to study effects of PFHxS during different stages of early zebrafish development. *Sci. Total Environ.* 808, 151739. <https://doi.org/10.1016/j.scitotenv.2021.151739>.
- Ziarrusta, H., Ribbenstedt, A., Mijangos, L., Picart-Armada, S., Perera-Lluna, A., Prieto, A., Izagirre, U., Benskin, J.P., Olivares, M., Zuloaga, O., Etxebarria, N., 2019. Amitriptyline at an environmentally relevant concentration alters the profile of metabolites beyond monoamines in gilt-head bream. *Environ. Toxicol. Chem.* 38, 965–977. <https://doi.org/10.1002/etc.4381>.